



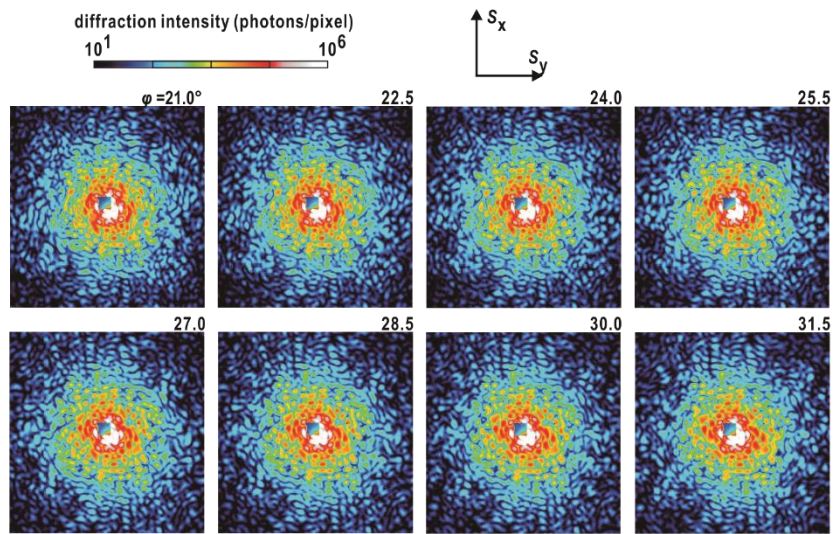
JOURNAL OF  
SYNCHROTRON  
RADIATION

**Volume 25 (2018)**

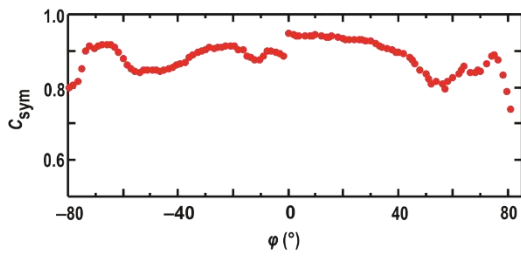
**Supporting information for article:**

**Diffraction apparatus and procedure in tomography X-ray diffraction imaging for biological cells at cryogenic temperature using synchrotron X-ray radiation**

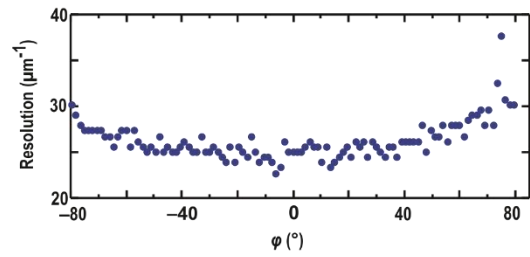
**Amane Kobayashi, Yuki Takayama, Koji Okajima, Mao Oide, Takahiro Yamamoto, Yuki Sekiguchi, Tomotaka Oroguchi, Masayoshi Nakasako, Yoshiki Kohmura, Masaki Yamamoto, Takahiko Hoshi and Yasufumi Torizuka**



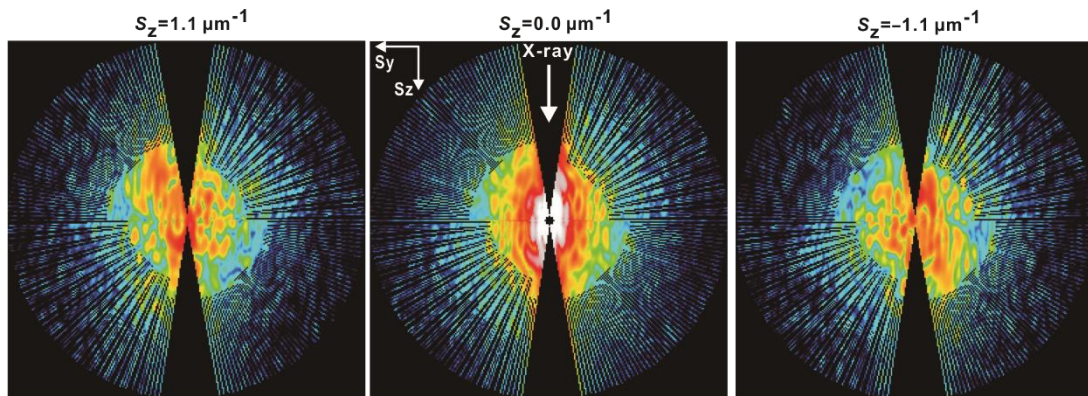
(a)



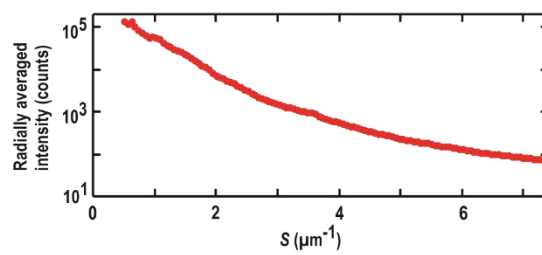
(b)



(c)



(d)



(e)

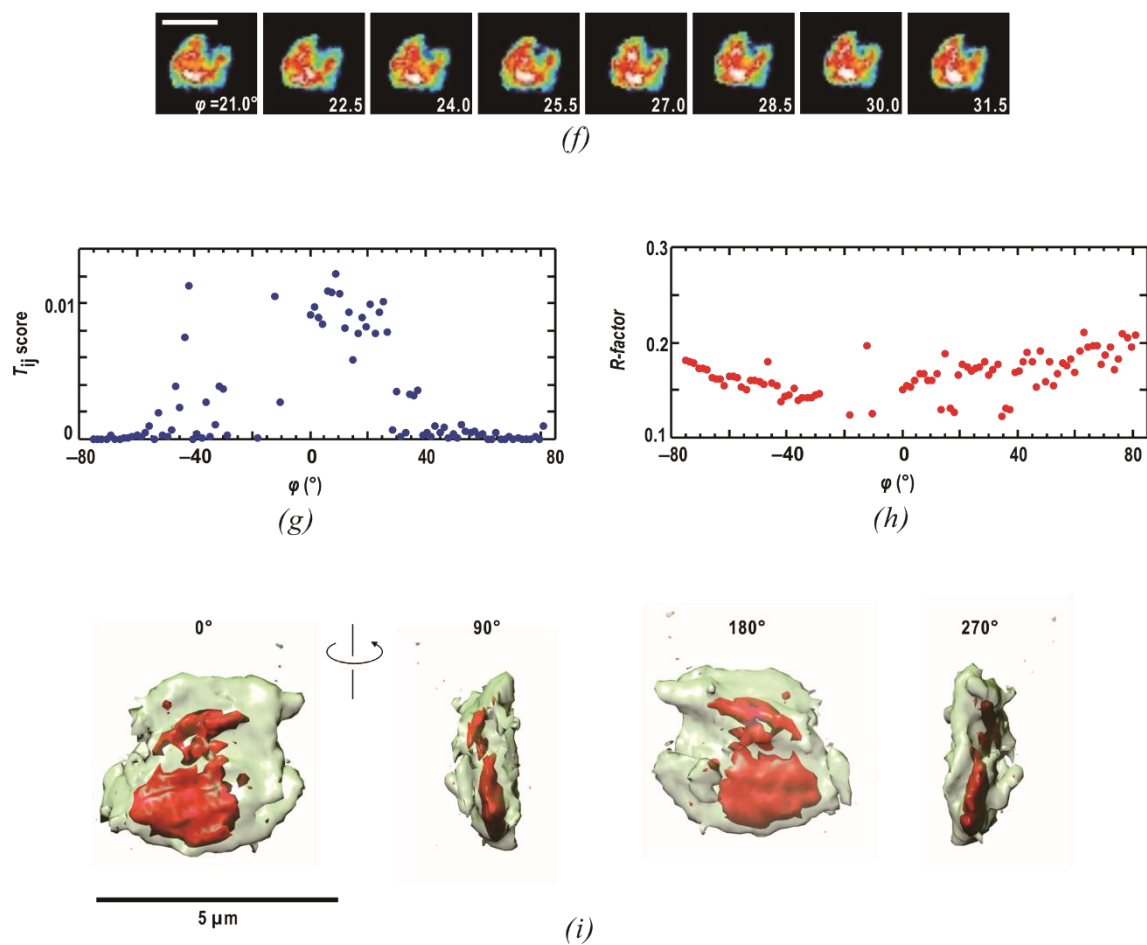


**Figure S1** (a) Series of diffraction patterns from *S. cerevisiae* during a successive  $1.5^\circ$  rotation around  $\phi=27^\circ$ . The resolution at the edge is  $6.31 \mu\text{m}^{-1}$ , corresponding to 158 nm in real space. The variation of  $C_{\text{sym}}$  values (b) and maximum resolution (c) plotted against the rotation angle. The  $C_{\text{sym}}$  values of most diffraction patterns were in the range of 0.8-0.95 except  $70^\circ < \phi$  (Fig. 8(b)). Large speckle sizes tend to result in higher  $C_{\text{sym}}$  values, probably because of a high sampling ratio. The maximum resolution kept at 22-38  $\mu\text{m}^{-1}$  implied little radiation damage to the cell. (d) The distribution of diffraction intensity in the  $S_y$ - $S_z$  planes at  $S_x=1.1$  (left panel), 0.0 (center), and  $-1.1 \mu\text{m}^{-1}$  (right). The resolution at the edge is  $14.7 \mu\text{m}^{-1}$ . The reconstructed 3D distribution of the diffraction intensity was almost centrosymmetric. (e) The resolution-

dependent variation of radially averaged diffraction intensity. The radially averaged diffraction intensity reached a value of  $10^5$  in the small-angle region and decreased gradually to  $10^2$ . (f) Projection electron density maps retrieved from the diffraction patterns in panel (a) at resolutions of 136 nm. The scale bar is 3  $\mu\text{m}$ . The density maps in the successive series of rotation were similar to each other with respect to the sizes, shapes and internal structures. The variation of  $T_{ij}$  (g) and crystallographic  $R$ -factor (h) values of the PR map from each diffraction pattern are plotted against the rotation angle. The similarity scores  $T_{ij}$  were very small, and crystallographic  $R$ -factors were less than 0.2. These results suggested the success of PR calculations and the selection of the most probable maps. (i) Four views of 3D electron density maps of *S. cerevisiae* reconstructed by the 3D PR method. The maps are contoured to demonstrate the cell envelop and high density regions. The model is illustrated as Fig. 8(c) of the main text.